Sensitive Stripping Voltammetric Determination of Pb (II) in Soil Using a Bi/single-walled Carbon Nanotubes-Nafion/ionic Liquid Nanocomposite Modified Screen-Printed Electrode

Ning Liu[1,2], Guo Zhao[3] and Gang Liu[1,2,]*

[1] Key Lab of Modern Precision Agriculture System Integration Research, Ministry of Education of China, China Agricultural University, Beijing, 100083, PR China
[2] Key Lab of Agricultural Information Acquisition Technology, Ministry of Agricultural of China, China Agricultural University, Beijing, 100083, PR China
[3] College of Engineering, Nanjing Agricultural University, Nanjing, 210031, PR China
[*]E-mail: pac@cau.edu.cn

In this study, Single-Walled Carbon Nanotubes (SWCNTs)-Nafion-Ionic Liquid (IL) composite modified Screen-Printed Electrode (SPE) (SWCNTs-Nafion/IL/SPE) was developed for the sensitive detection of trace Pb (II) in soil using Square Wave Anodic Stripping Voltammetry (SWASV) technique. The Bi/SWCNTs-Nafion/IL/SPE sensor was fabricated by the in-situ plating of bismuth ions on the SWCNTs-Nafion/IL/SPE surface. The morphologies and electrochemical properties of this modified SPE were characterized by Scanning Electron Microscopy (SEM), Cyclic Voltammetry (CV), Electrochemical Impedance Spectroscopy (EIS) and SWASV. The experimental parameters, such as pH value, Bi(III) concentration, deposition potential and deposition time, were optimized. The specific surface area and electron transfer capacity of the modified SPE were improved by the presence of SWCNTs, and the abilities of cation-exchange and metal ions pre-concentration were further enhanced by Nafion. Moreover, the existence of IL increased the conductivity of the composite. The detection limit of the developed sensor was 0.1 μg/L (S/N = 3) in the range of 1.0 to 100.0 μg/L for Pb (II). Finally, the Bi/SWCNTs-Nafion/IL/SPE was applied for detecting Pb (II) in real soil samples and the average recovery of 95.12% was obtained with satisfactory results.

1. INTRODUCTION

Lead is a non-essential biological element with high-potential toxicity, mobility, and persistence. Anthropogenic processes, such as fertilizer application and waste water irrigation, have greatly increased Pb content in the soil environment [1,2]. Those Heavy Metals Ions (HMIs)

accumulating in soil can harm to human health by eating crops grown in soil containing heavy metals [3]. Therefore, the rapid, accurate and reliable detection of toxic HMIs in soil has great significance.

Several analytical techniques have been developed for determining HMIs, such as Atomic Absorption Spectroscopy (AAS) [4], Inductively Coupled Plasma-atomic Emission Spectrometry (ICP-AES) [5], Flameless Atomic Absorption Spectrophotometry (FAAS) [6] and Inductively Coupled Plasma-Optical Emission Spectrometry (ICP-OES) [7]. These methods possess the high sensitivity and a low detection limit, but they are always associated with many disadvantages, for instance time-consuming, expensive, and complex, which restrict their practical applications and HMIs determination onsite.

Anodic Stripping Voltammetry (ASV) as one of the typical electrochemical techniques has received increasing attention to the detection of HMIs because of its easy operation, rapid response, high sensitivity and high selectivity [8, 9]. Over the past decades, Screen-Printed Electrodes (SPEs) have been widely employed to analyze HMIs combining with ASV technique due to its excellent performances, such as low background current [10], easy modification [11], disposability and low-cost [12]. However, SPEs still have some shortcomings, such as low electron transfer rate and small specific surface area, which can be made up via modification using advanced materials.

In recent years, nanomaterials are widely employed for the modification of electrodes to improve the electrochemical properties, and further enhance the chemical analytical abilities [13, 14, 15]. The bismuth film possesses many excellent electrochemical properties, including low toxicity [16], wide electrochemical window [17], and the ability of forming alloys with target HMIs to reduce the activation energy of HMIs electronical reduction [18], and it has become a popular material to modify the Working Electrode (WE) for determining HMIs. The method of in-situ plating of bismuth film on an electrode surface was the mostly applied when using ASV [19, 20]. The way of in-situ method was that a number of bismuth ions were added to the sample solution, then the Bi ions, together with target HMIs, were electrodeposited on the WE surface by a reduction potential [21]. SWCNTs were widely applied to modify WE due to its excellent dispersibility in organic solvent [22], large specific surface area [23], and good conductivity [24]. Previous literatures had reported that the electrodes modified by SWCNTs combining with metal nanoparticles, such as Gold Nanoparticles (AuNPs) and Silver Nanoparticles (AgNPs), were superior sensors for the measurement of trace HMIs [25, 26]. For example, Molinero et al. developed an AuNPs/SWCNTs-enabled SPE sensor to detect Pb (II) [27]. With the addition of AuNPs or AgNPs, the conductivity of the developed sensor was further improved. However, these precious metals possess many shortcomings, such as expensive price and inherent toxicity, which will limit practical application and disposability of SPEs.

In addition, IL has been widely applied in the modification of electrochemical sensors because of its outstanding performances of high electron conductivity [28] and low volatility [29] and environmental friendliness [30]. Many studies reported that IL could be used in various working electrodes and be combined with substance, such as organic nanotubes and metal nanoparticles [31, 32, 33]. For example, Edgar et al. [34] proposed a screen-printed carbon electrode modified with the SWCNTs and IL for the determination of uric acid and dopamine with the detection limit of 0.17μmol/L for uric acid and 0.16μmol/L for dopamine, respectively. Additionally, Nafion possesses a negatively charged skeleton, which can improve the cation-exchange capacity of an electrode surface

[35]. Moreover, Nafion has the ability to enhance the anti-interference performance of the electrode surface and strengthen the mechanical stability on the modified layer of the electrode surface [36].

Considering the above content, in this study, we reported an environment friendly electrochemical sensor based on a SPE modified with Bi/SWCNTs-Nafion/IL composite for the sensitive determination of trace Pb(II) using SWASV. The synergistic effects of bismuth catalytic capacity, the high conductivity of IL, the large specific surface area of SWCNTs, as well as the good cation-exchange abilities of Nafion resulted in an excellent electrochemical performance of the proposed Bi/SWCNTs-Nafion/IL/SPE. Since the electrode modification materials were non-polluting, this sensor was environmentally friendly. Finally, the practicality of the developed sensor was tested by the Pb(II) determination in real soil samples. The electrochemical detection process of Pb(II) is shown in Figure 1.
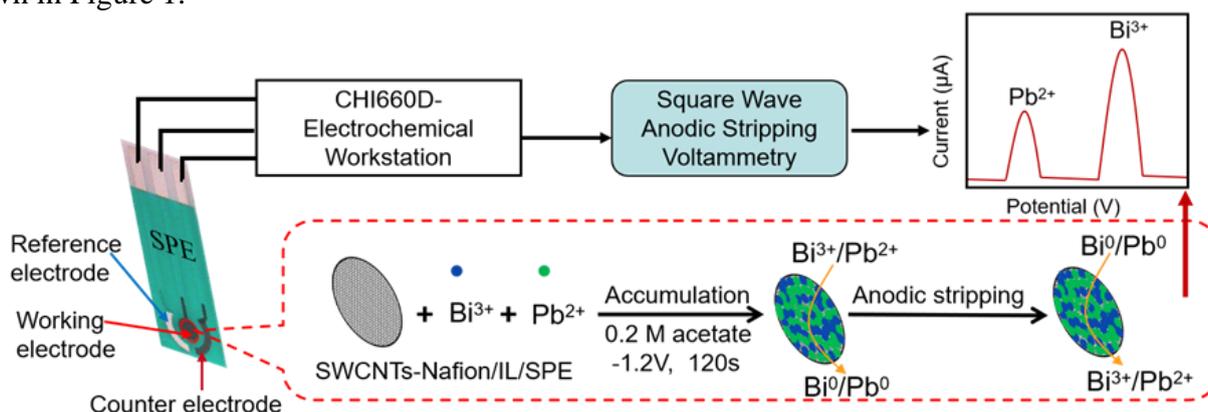
Figure 1. Schematic illustration of the electrochemical detection of Pb^{2+} using the Bi/SWCNTs-Nafion/IL/SPE

2. MATERIALS AND METHODS

2.1. Reagents and instruments

Standard solutions of Pb(II) and Bi(III) (1mg/mL) were purchased from National Standard Reference Materials Centre of China and diluted as required. Acetate buffer solution (0.2M) was used as the electrolyte for the electroanalysis of Pb (II). SWCNTs (aqueous dispersion solution, 0.15 wt %) were obtained from Shenzhen Nanotech Port Co., Ltd. (Shenzhen, China). Nafion (1.0 wt%) and IL were purchased from Aldrich (Sigma-Aldrich, USA). Nafion was diluted to 0.1 wt % with pure ethanol before use. Millipore-Q water (18.2MΩ) was applied for all experiments.

SEM was performed under a JEOL JSM-6701F (Japan) field-emission scanning electron microscope. The electrochemical measurements and analysis, including EIS, CV, and SWASV were carried out using a CHI660D electrochemical workstation (Shanghai CH Instruments, China). The SPE was purchased from the Shanghai Branch (Shanghai, China) of Yangtze River Delta System Biological Cross Science Research Institute Co., Ltd. The Reference Electrode (RE) was composed of Ag/AgCl paste, the Counter Electrode (CE) and WE were the modes of graphite paste, which were used as a

three-electrode system. A 30 mL beaker was used as an electrolytic cell for all electrochemical measurements. A magnetic stirrer was used to stir the test solution during the deposition process.

2.2. Preparation of SWCNTs-Nafion/IL/SPE

Briefly, the fabrication process of SWCNTs-Nafion/IL/SPE can be described as follows:

The IL was diluted 100-fold with ethanol to obtain the 1% IL mixture. Then, 1.0% Nafion was diluted with the ethanol solution to obtain the 0.1% Nafion solution. SWCNTs aqueous solution and 0.1% Nafion were mixed with a volume ratio of 1:5 to obtain SWCNTs-Nafion mixture. All above mixture solutions had been sonicated for 30 min to ensure uniform dispersion. After that, 6 μL of the 1% IL was pipetted onto the WE surface and solidified in an oven at 60 °C to obtain the IL/SPE. Finally, 6 μL of the SWCNTs-Nafion suspension was coated on the IL/SPE and solidified at 60°C to obtain the SWCNTs-Nafion/IL/SPE.

2.3. Electrochemical detection of Pb(II)

SWASV measurements of Pb (II) were performed in acetate buffer solution (0.2 M, optimal pH 5.5) containing 1200 μg/L Bi (III) (optimal Bi (III) concentration) using Bi/SWCNTs-Nafion/IL/SPE. During deposition, a potential of -1.2 V (optimal potential) (vs. Ag/AgCl) had been applied to the electrode for 120 s (optimal deposition time) with stirring to reduce the HMIs. Then, equilibration had been carried out for 10 s after that a stripping voltammogram was performed in a potential range of -0.7 V to -3.5 V without stirring during equilibration and stripping. The values of 5mV, 25Hz, and 25mV were used for the step amplitude, frequency, and pulse amplitude, respectively. An activation process had been initiated in the acetate buffer to clean the electrode surface and remove residual bismuth and heavy metals using a constant negative potential (-0.4 V) for 240s after each SWASV measurement.

2.4. Soil sample preparation

The extract solutions of soil samples were prepared according to the description in previous literature [37] and [38]. Briefly, the preparation procedure of the soil samples is summarized as follows: first, the soil samples were placed in an oven to dry for 2 h. Second, the soil samples were pulverized on a portable soil crusher and subsequently sieved through a 200 μm sieve. Third, 30 mL of 0.2 M acetate buffer (pH 5.5) was mixed with a 2 g soil sample with strong shaking. After that, the soil mixture solution samples were subjected to centrifugal sedimentation process. Finally, the supernatant was filtered by a membrane to remove micro-impurities from the solutions, and then 20 mL of the extract solution was loaded into an electrolyte cell for subsequent SWASV measurement.

3. RESULTS AND DISSCUSSION

3.1. Morphology characteristics of the modified electrodes

The surface morphologies of different modified electrodes were characterized by SEM. The SEM image of bare SPE is shown in Figure 2A, displaying the uneven surface with many holes formed by multilayer graphite. The SEM image of IL/SPE (Figure 2B) shows that the surface is smooth and flat due to the filling of ionic liquid. Furthermore, the formed IL film would improve the electron transporting ability of the SPE [39]. The SEM images of the SWCNTs-Nafion/IL/SPE at two different magnifications are shown in Figure 2C and Figure 2D, appearing a uniformly and densely granular distribution structure because of the effective dispersion of SWCNTs under the action of Nafion. The dense multilayer distribution of SWCNTs enabled a large specific surface area of modified electrode, facilitating the generation and growth of bismuth nanoparticles to form a sufficient bismuth film, which further increased the number of active sites and the preconcentration amount of target Pb (II).
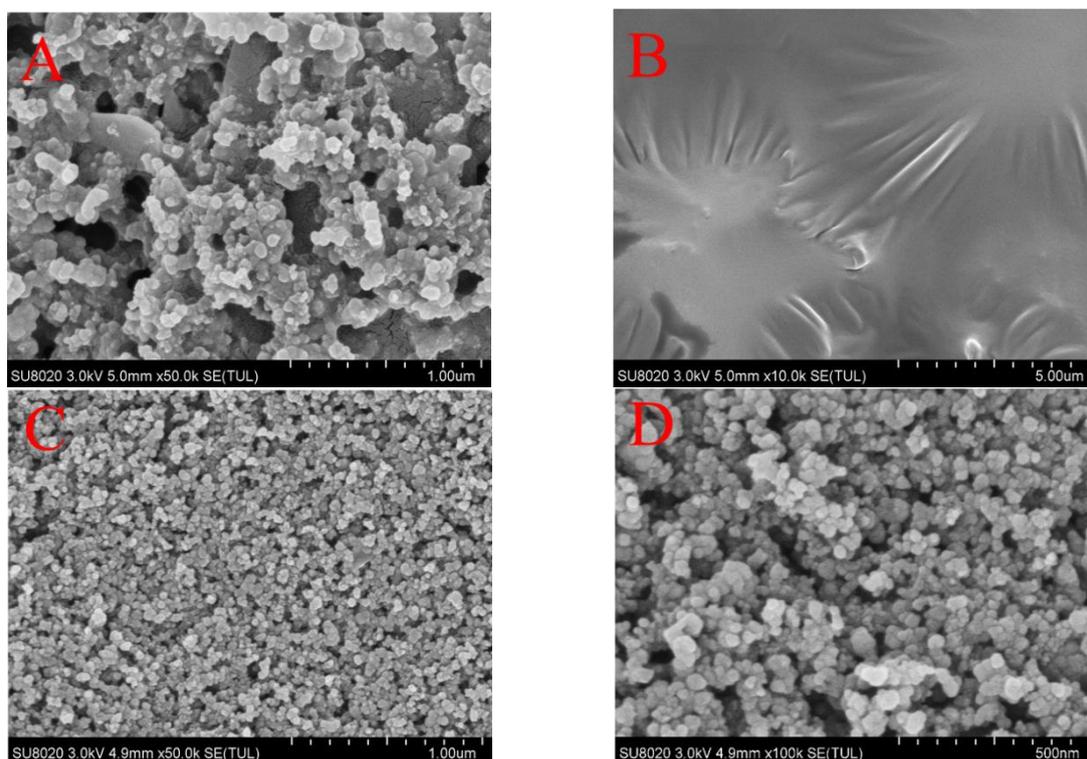
Figure 2. SEM images of (A) bare SPE, (B) IL/SPE, and (C, D) SWCNTs-Nafion/IL/SPE at two different magnifications

3.2 Electrochemical properties of the modified electrodes

The electrochemical properties of different modified electrodes were investigated by CV using $[Fe(CN)_6]^{3-/4-}$ as a redox probe. The CV results of three modified electrodes in a 5.0 mM $[Fe(CN)_6]^{3-/4-}$ and 0.1 M KCl mixture solution are shown in Figure 3A. The redox current peaks of $[Fe(CN)_6]^{3-/4-}$ for the IL modified SPE (IL/SPE), as shown in Figure 3A(b), were obviously greater than bare SPE (Figure 3A(a)), and together with a smaller peak-peak separation, which demonstrated that the IL can

greatly enhance the electron transfer capacity of the electrode surface. Under the same conditions, the CV result of the SWCNTs-Nafion/IL/SPE is shown in Figure 3A(c). The amplitude of the redox peaks (the peak-peak separation) was significantly smaller (larger) than those of the SPE and IL/SPE due to the severe non-conductivity of Nafion, although the SWCNTs owned good electron transfer capacity.

The electron transfer capacities of the different modified electrodes were further investigated by EIS, as shown in Figure 3B. In the Nyquist diagram, the diameter of the semicircle at higher frequencies was approximately equal to the interfacial charge transfer resistance (Rct) [40]. A well-defined semicircle was observed for IL/SPE (Rct $\approx$ 1972 kΩ, Figure 3B(b)), and it was smaller than that for the bare SPE (Rct $\approx$ 6324 kΩ, Figure 3B(a)), which revealed the small Rct value of the IL/SPE. The result, which was in agreement with the CV results, could be attributed to the good electron transfer capacity of IL. However, an obviously large semicircle diameter, which demonstrated that the SWCNTs-Nafion/IL/SPE (Rct $\approx$ 45980 kΩ) possessed the greater interfacial Rct than bare SPE and IL/SPE, could be found in Figure 3B(c). Above results showed that the electron transfer kinetics of the redox probe at the SWCNTs-Nafion/IL/SPE were hindered, which was due to the existence of non-conductive Nafion and the repulsion of negative charge skeleton of Nafion to the anions of the redox probe.
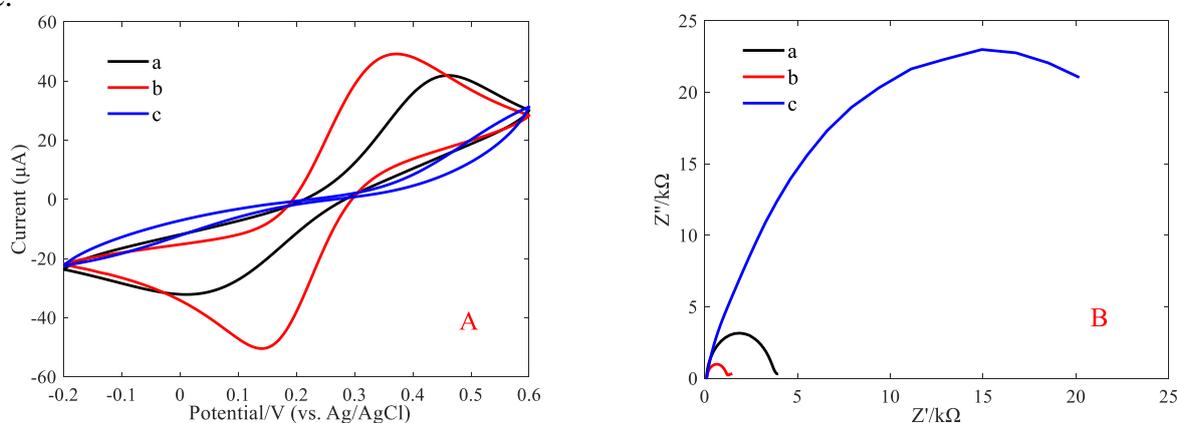
Figure 3. (A) CV curves of 5 mM [Fe(CN)$_6$]$^{3-/4-}$ in 0.1 M KCl solution: (a) SPE, (b) IL/SPE, (c) SWCNTs-Nafion/IL/SPE. Scan rate: 50 mV/s, and (B) EIS results of the (a) SPE, (b) IL/SPE, (c) SWCNTs-Nafion/IL/SPE in 5 mM [Fe(CN)$_6$]$^{3-/4-}$ in 0.1 M KCl solution.

3.3 Optimization of experimental conditions

To obtain the best sensitivity for the SWASV detection of Pb(II) using the Bi/SWCNTs-Nafion/IL/SPE, the relevant SWASV parameters, including the Bi(III) concentration, pH value of the supporting electrolyte, deposition potential, and deposition time, were optimized as shown in Figure.4.

The effect of the Bi (III) concentration on the stripping responses of Pb (II) was studied, as shown in Figure 4A. The peak currents were enlarged with the Bi (III) concentration increasing from 0 to 1200 μg/L, and then reduced gradually. The reason was that a small amount of Bi (III) was not enough to form an alloy with the Pb (II) to reduce the activation energy required for Pb (II) electrochemical reduction. However, if the Bi (III) concentration was too high, it would occupy lots of active sites on the WE surface, which influenced the reduction reaction of Pb (II). Therefore, the

optimal Bi (III) concentration was 1200 μg/L. Figure 4B showed the effects of pH value in the range of 3.5-6.5 on the peak currents of Pb (II). The maximum peak current of SWASV appeared at pH 5.5. Consequently, the subsequent experiments were conducted at pH 5.5. The effect of the deposition potential on the peak currents of Pb (II) over a range of -1.6 V to -0.8 V after electrochemical accumulation for 120s was studied, as shown in Figure 4C. The highest peak current was obtained at -1.2 V for the Pb (II) detection. Therefore, the -1.2 V was chosen as the optimal accumulation potential for Pb (II) pre-concentration. Figure 4D demonstrated the influence of deposition time on the stripping responses of Pb (II). The peak currents of Pb (II) using Bi/SWCNTs-Nafion/IL/SPE increased gradually as the deposition time increasing from 60 s to 420 s. However, the increase of peak current in the range of 120 s-420 s was slower than those of 60 s-120 s. Regarding the detection sensitivity and efficiency, the deposition time of 120 s was applied in subsequent SWASV detection.
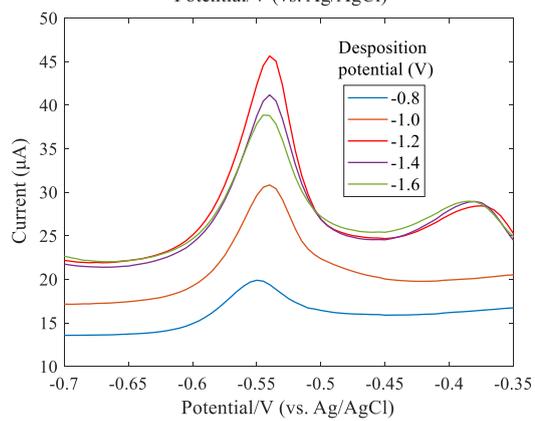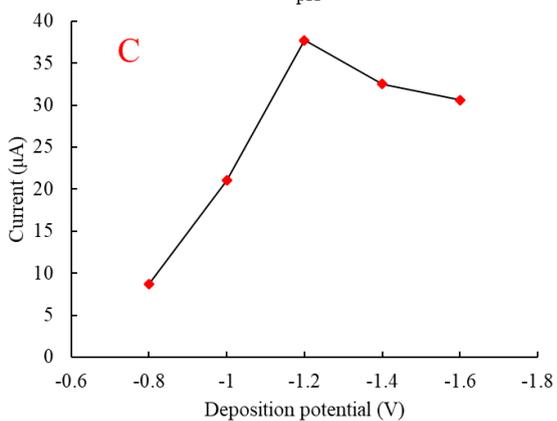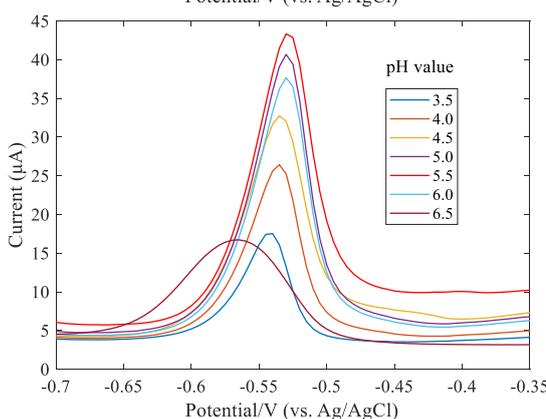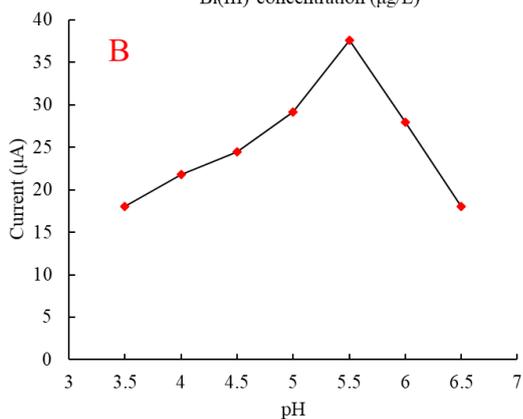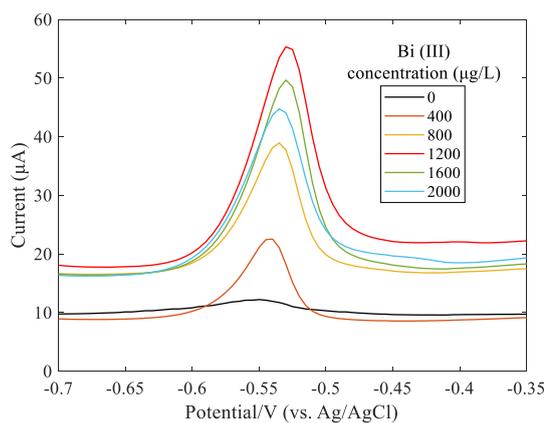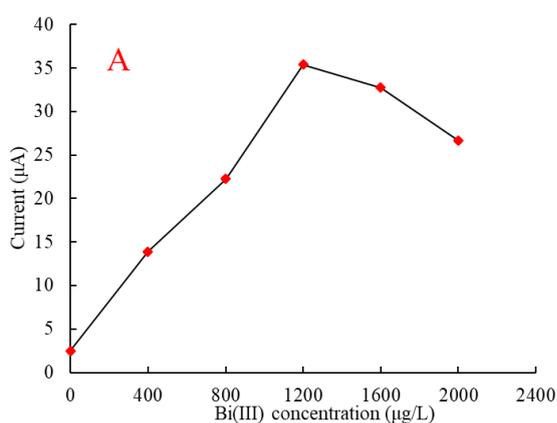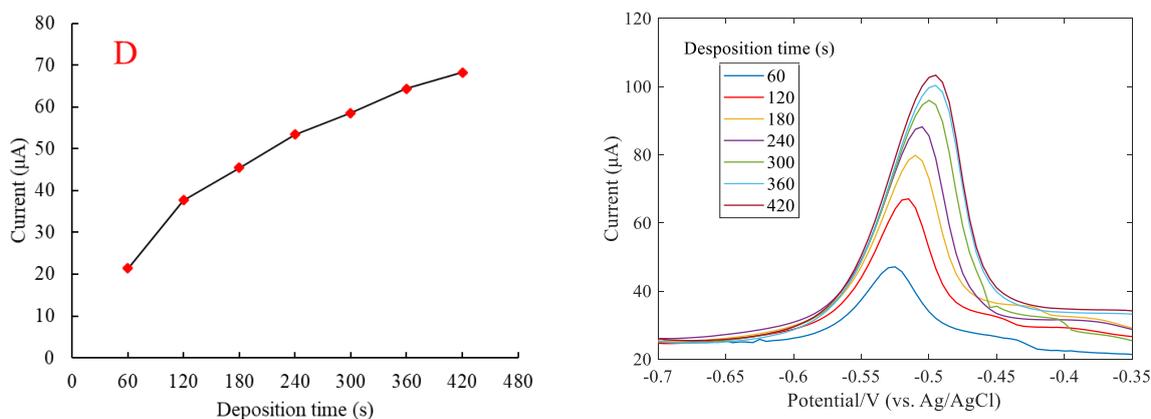
Figure 4. Effects of the (A) Bi(III) concentration, (B) pH, (C) Deposition potential, (D) Deposition time on the stripping peak currents of 20 μg/L Pb(II).

3.4 Stripping responses of various electrodes

The SWASV results of 10 μg/L Pb(II) on three modified electrodes, including Bi/SPE, Bi/IL/SPE, and Bi/SWCNTs-Nafion/IL/SPE, were studied in a potential range from -0.7 to -0.35 V under the optimized experiment conditions, as shown in Figure 5. The stripping current signal of Pb (II) on the SPE was the lowest (Figure 5(a)). In contrast, the amplitude of stripping current was larger toward Pb(II) on the IL/SPE (Figure 5(b)), which attributed to the excellent electric conductivity of IL. The SWCNTs-Nafion/IL/SPE (Figure 5(c)) exhibited the highest sensitivity toward Pb (II). Such improvement could be attributed to two respects. Firstly, the conductive SWCNTs could further improve the electron transfer rate on the WE surface. Moreover, the existence of SWCNTs effectively increased the specific surface area of the modified electrode, which resulted in a great enhancement of the electrical reduction of Pb(II) and the homogenous distribution of alloys of Bi (III) and Pb (II). Secondly, the negatively charged polymeric membrane composed of Nafion with sulfonate groups could serve as a cation exchanger that promoted the pre-concentration of Pb (II) on the Bi/SWCNTs-Nafion/IL/SPE surface, which further improved the deposition efficiency of Pb (II) on the WE surface [13]. Furthermore, Nafion could facilitate SWCNTs separation and prevent aggregation of SWCNTs. The synergistic effect of the high conductivity of IL, the homogenous distribution of SWCNTs in Nafion, and the negatively charged skeleton of Nafion led to an excellent electrical deposition capability of the Bi/SWCNTs-Nafion/IL composite.
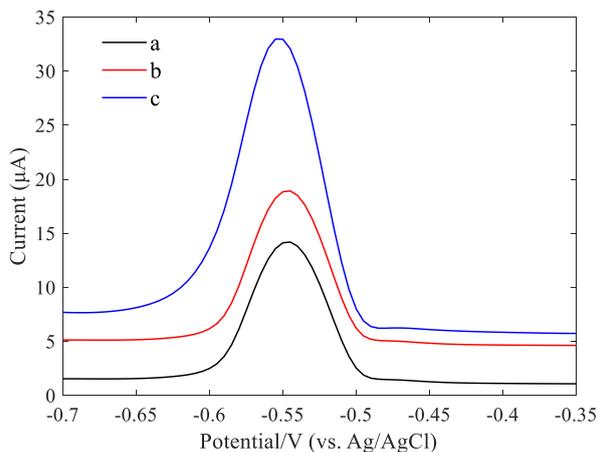
Figure 5. SWASV results of 10 μg/L Pb(II) in 0.2 M acetate buffer using the (a) Bi/SPE; (b) Bi/IL/SPE; (c) Bi/SWCNTs-Nafion/IL/SPE under optimized experiment condition.

In addition, the results shown in Figure 5 did not contradict those shown in Figure 3, because Figure 3 revealed that the electron transfer capacity of SWCNTs-Nafion/IL/SPE was poor, but this capacity could not uniquely determine the detection performance of the modified electrode. Except for electronic conductivity, other factors, such as the ability of absorbing and accumulating heavy metal ions, might more critically affect the sensing performance of electrochemical sensors. Additionally, other researchers also observed the same phenomena. For example, Zhao et al. [9] developed a $(BiO)_2CO_3$@SWCNTs-Nafion composite-modified glassy carbon electrode to detect the concentration of Pb (II) and Cd (II), and achieved the best sensitivity using this electrode with the lowest electronic conductivity. Moreover, Xu [41] proposed a non-conductive nanomaterial that improved the detection performance of HMIs.

3.5 Stability analysis of Bi/SWCNTs-Nafion/IL/GCE

The stability of the Bi/ SWCNTs-Nafion/IL/SPE was tested by six repetitive detections of 20 μg/L Pb (II) in 0.2 M acetate buffer (pH 5.5), as shown in Figure 6. The peak currents of the Pb (II) on the Bi/SWCNTs-Nafion/IL/SPE were reproducible, with a Relative Standard Deviation (RSD) of 1.06%. The Bi/SWCNTs-Nafion/IL/SPE displayed an excellent stability for detection of Pb (II) under the optimized experiment condition.
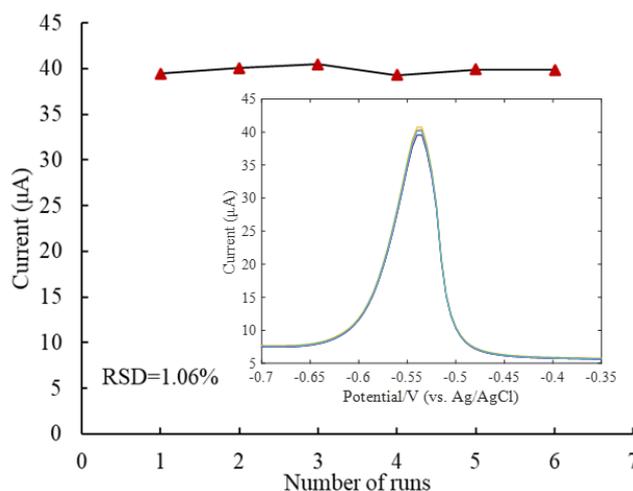
Figure 6. Six SWASV results of 20 µg/L Pb (II) on the Bi/SWCNTs-Nafion/IL/SPE in 0.2 M acetate buffer (pH 5.5).

3.6 Analytical performance of Bi/SWCNTs-Nafion/IL/SPE

　　　　Under the optimized condition, several measurements were performed using SWASV method to build a linear calibration curve for Pb(II) over a concentration range of 1-100 µg/L. A series of SWASV curves of Pb(II) at different concentrations are shown in Figure 7. The increasing rate of stripping peak current in the Pb(II) concentration range of 1-10 µg/L (Figure 7A) was larger than those of 10-100 µg/L (Figure 7B). The reason might be that the number of active sites on electrode surface was much higher than that of Pb(II), so that the detection sensitivity was higher, as compared with the low Pb(II) concentration. And Pérez-Ràfols et al. [42] also observed the same phenomenon.
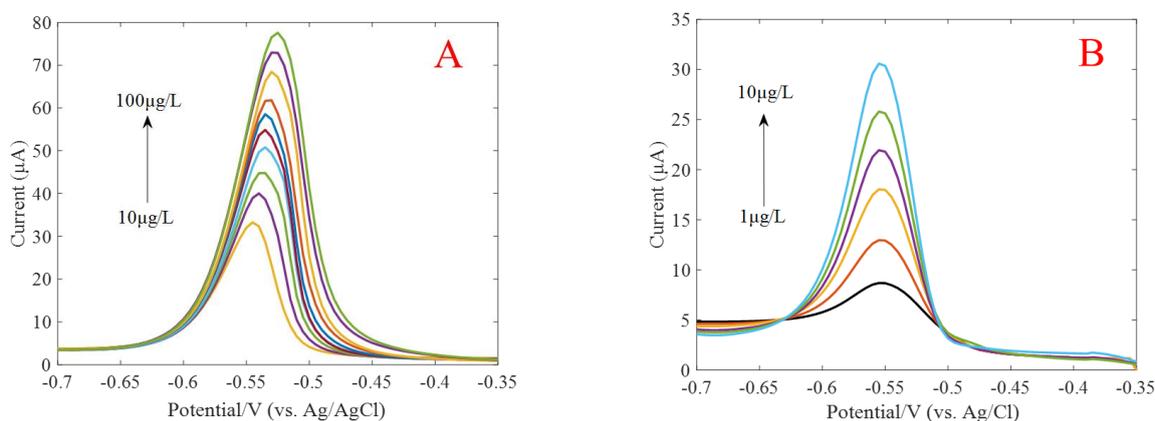
Figure 7. SWASV curves for concentrations of (A) 10, 20, 30, 40, 50, 60, 70, 80, 90 and 100 µg/L, (B) 1, 2, 4, 6, 8 and 10 µg/L for Pb (II)

　　　　As explained in Figure 7, the linear calibration model was respectively established over a Pb(II) concentration range of 1-10 µg/L and 10-100 µg/L, as shown in Figure 8. The calibration model and square values of correlation coefficients were y = 2.8369x + 2.9025 (x: µg/L, y: µA, R^2=0.9914) for 1-10 µg/L, and y = 0.4811x + 27.8450 (x: µg/L, y: µA, R^2=0.9959) for 10-100 µg/L, respectively. The

detection sensitivities were 2.8369 µA (µg/L)$^{-1}$ for 1-10µg/L, and 0.4811 µA (µg/L)$^{-1}$ for 10-100µg/L. The detection limits (S/N = 3) were 0.1 µg/L for 1-10 µg/L, and 0.58 µg/L for 10-100 µg/L.

The peak stripping current was 31.75 µA at concentration (10 µg/L) of Pb (II) according to the SWASV measurement results. Therefore, the model y = 2.8369x + 2.9025 was applied to calculate the Pb (II) content if the peak current was below 31.75 µA, otherwise the model y = 0.4811x + 27.8450 was used. As we all know, the detection limit was the lowest target ions concentration that could be detected using sensors. Thence, the detection limit of the developed Bi/SWCNTs-Nafion/IL/SPE, in this research, was 0.10 µg/L (S/N = 3).
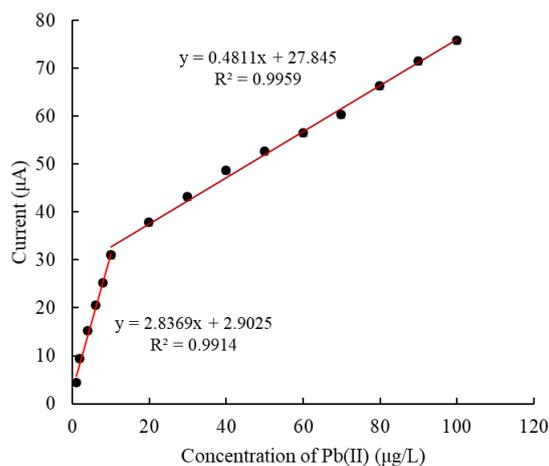
Figure 8. The calibration model of stripping peak currents and the concentrations of Pb (II)

A comparison of the main detection performance of Bi/SWCNTs-Nafion/IL/SPE developed in this study and other SPEs in previous reports is presented in Table 1. It could be found from Table 1 that the SPE modified by Bi/SWCNTs-Nafion/IL composite possessed the lowest detection limit for Pb(II), which demonstrated that performance of the proposed Bi/SWCNTs-Nafion/IL/SPE was better than previous works.

Table 1. Comparison of different SPEs for determination of Pb(II).

Electrode	Technique	Linear range (µg/L)	Detection limit	Reference
AgNPs/SPCNFE	SWASV	6.6-53.5	1.98	[42]
Antimony film/SPCE	DPASV	10-90	0.25	[43]
GR/l-cysteine/Bi/SPE	SWASV	10-50	0.56	[44]
AuNPs/SPE	SWASV	2.0-500.0	4.4	[45]
CNPs-BiNPs/SPE	ASV	6.6-53.5	1.98	[46]
SWCNTs/IL/SPE	SWASV	1.0-60.0	0.12	[47]
GR/PANI/PS/SPE	SWASV	10.0-500	4.43	[48]
Bi/SWCNTs-Nafion/IL/SPE	SWASV	1-100	0.10	This work[1]

[1]AgNPs-SPCNFE: Ag-nanoparticles/carbon nanofiber modified screen-printed electrode; Antimony film-SPCE: Antimony film modified screen-printed carbon electrode; GR/l-cysteine/Bi/SPE: reduced

grapheneoxide/ L-cysteine/bismuth composite modified SPE; AuNPs/SPE: Au-nanoparticles modified SPE; CNPs-BiNPs/SPE: Carbon nanoparticles-bismuth nanoparticles composite modified SPE; SWCNTs/IL/SPE: Single-walled carbon nanotubes/ionic liquid composite modified SPE; GR/PANI/PS/SPE: Graphene/polyaniline/polystyrene fibers modified SPE.

3.7 Interference analysis of Bi/ SWCNTs-Nafion/IL/GCE

Under an optimized experimental condition, the influence of various non-target metal ions that may be present in real soil extraction solution samples such as Zn^{2+}, As^{3+}, Cr^{2+}, Cd^{2+}, Hg^{2+}, and Cu^{2+} on the peak currents of Pb (II) was studied at a concentration ratio of 100:1 (interfering ions: Pb (II)). The interference level of different ions on with Pb (II) measurements was expressed by the RSD, as shown in Figure 9. The results showed that except for Cu (II), the RSDs of other non-target ions were all blow 10%. Therefore, Cu (II), as the greatest interference ion, had a significantly negative influence on the stripping peak current of Pb (II), which decreased the stripping peak current of Pb (II) approximately 27.26%. The reason was that Cu (II) could compete with the active sites on the electrode surface with Pb (II). However, the interference of Cu (II) on the Pb (II) sharply decreased (from 27.26% to 0.66%), as shown in Figure 9, when the ferricyanide ($K_4Fe(CN)_6$) was added to the samples at the same concentration with Cu (II). This change was because an insoluble copper-ferricyanide complex was formulated with the help of a ligand [49].
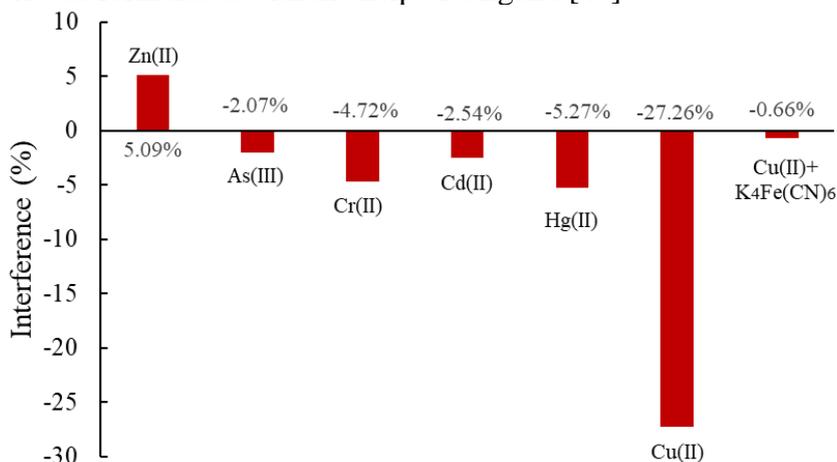
Figure 9. Study of peak current interference from ions at concentrations 100-fold same to that of Pb (II) (20 μg/L)

3.8 Application to soil sample determination

In order to further test the practicability of the developed Bi/SWCNTs-Nafion/IL/SPE, this modified electrode was applied to determinate Pb (II) in real soil samples. The soil samples were prepared according to Section 2.4, and the measurements were conducted using the standard addition method under optimal experiment conditions. According to the Section 3.7, the ferricyanide was added to the extract solution of the sample to eliminate the interference of Cu (II) on the stripping signals of

Pb (II). Because the pKsp value of $Cu_2[Fe(CN)_6]$ was 15.89, this copper-ferricyanide complex was insoluble [50]. A battery of potassium ferricyanide was evaluated. The results revealed that a concentration of 0.1mM $K_4[Fe(CN)_6]$ was sufficient to eliminate the influence due to natural existing Cu (II) in the soil samples. Therefore, 0.1 mM $K_4[Fe(CN)_6]$ was spiked in the sample extract solution before the measurement. The detection results of Pb (II) are presented in Table 2. The average recovery of Pb (II) was 95.12%, which revealed that the detection results were satisfactory. The application experiments demonstrated the feasibility of applying the Bi/SWCNTs-Nafion/IL/SPE for detecting Pb (II) in real soil samples.

Table 2. Results of the detection of Pb(II) in soil sample extracts.

Sample no.	Added (µg/L)	Detected by SWASV(µg/L)[1]	Recovery (%)
	-	2.73 ± 0.19[2]	-
1	5	7.31 ± 0.09	91.56%
	10	12.80 ± 0.23	100.78%
	-	5.71 ± 0.29	-
2	10	14.92 ± 0.23	92.14%
	15	20.21 ± 0.10	96.67%
	-	5.63 ± 0.18	-
3	15	19.74 ± 0.25	94.08%
	20	24.73 ± 0.17	95.48%

[1] Five times detection for each sample. [2] mean value ± standard deviation

4. CONCLUSIONS

In this study, we introduced a way to develop an environment friendly Bi/SWCNTs-Nafion/IL composite modified SPE for the Pb (II) detection. The characteristics of the Bi/SWCNTs-Nafion/IL/SPE were studied by SEM, CV, EIS, and SWASV. The Bi/SWCNTs-Nafion/IL/SPE displayed excellent electrochemical activity and the strong charge transfer capacity result from the existence of the conductive IL and SWCNTs. The large specific surface area of SWCNTs, the high ion exchange capacity and good antifouling ability of Nafion, as well as the catalytic property of the bismuth film for Pb (II) led to a high sensitivity and low detection limit for the determination of trace Pb (II), which also demonstrated good reproducibility and stability. Moreover, the practicability of the developed Bi/SWCNTs-Nafion/IL/SPE was verified by detecting the Pb (II) in real soil samples with a average recovery of 95.12%. This study reported a green, stable, and sensitive electrochemical sensor, which has great application prospects in the monitoring of HMIs in soil environment and so on.

References

1. Y. Jia, T. Zhao, N. Zhao, H. Wei, W. Zhang, and R. Qiu, *Chemosphere*, 225 (2019) 174.

2.   C. Bi, Y. Zhou, Z. Chen, J. Jia, and X. Bao, *Sci. Total. Environ.*, 619 (2018) 1349.
3.   L. Li, Y. Zhang, J. Ippolito, W. Xing, K. Qiu, and H. Yang, *Environ. Pollut.*, 257 (2020) 113641.
4.   Z. Wang, D. Wu, G. Wu, N. Yang, and A. Wu, *J. Hazard. Mater.*, 244 (2013) 621.
5.   K. Hassan, M.F. Mousavi, Y. Yamini, and M. Shamsipur, *Anal. Chim. Acta.*, 509 (2004) 89.
6.   T.Daşbaşı, Ş.Saçmacı, N. Çankaya, and C. Soykan, *Food Chemistry,* 203 (2016) 283.
7.   A.M. Massadeh, A.A. Alomary, S. Mir, F.A. Momani, and Y.A. Hadad, *Environ. Sci. Pollut. Res.*, 23 (2016) 13424.
8.   G. Zhao, H. Wang, and G. Liu, *Int. J. Electrochem. Sci.*, 12 (2017) 8622.
9.   G. Zhao, Y. Yin, H. Wang, G. Liu, and Z. Wang, *Electrochim. Acta*, 220 (2016) 267.
10. J. Wang, Z. Xu, M. Zhang, J. Liu, H. Zou, and L. W, *Talanta*, 192 (2019) 40.
11. M.I. González-Sánchez, B.G. Monedero, J. Agrisuelas, and J. Iniesta, *J. Electroanal. Chem.*, 839 (2019) 75.
12. L. Xiaoxue, Y. Yao, Y. Yibin, and P. Jianfeng, *TrAC, Trends Anal. Chem.*, 115 (2019) 187.
13. G. Zhao, and G. Liu, *Sens. Actuators, B*, 288 (2019) 71.
14. J. Huangxian, *Applied Materials Today*, 10 (2018) 51.
15. L. Xiaoxue, Y. Yao, Y. Yibin, and P. Jianfeng, *Trends Anal. Chem.*, 115 (2019) 187.
16. J. Liu, X. Yuan, Q. Gao, H. Qi, and C. Zhang, *Sens. Actuators, B*, 162 (2012) 384.
17. K. Domańska, and K.T. Rotko, *Anal. Chim. Acta*, 1036 (2018) 16.
18. S. Lee, S.K. Park, E. Choi, and Y. Piao, *J. Electroanal. Chem.*, 766 (2016) 120.
19. Y. Wang, Z. Liu, G. Yao, Zhu, X. Hu, and Q. Xu, *Talanta*, 80 (2010) 1959.
20. M. Marton, P. Michniak, M. Behul, V. Rehacek, A.V. Stanova, R. Redhammer, and M. Vojs, *Vacuum*, 167 (2019) 182.
21. C. Rojas-Romo, M.E. Aliaga, and V. Arancibia, *Microchem. J.*, 154 (2020) 104589.
22. R. Tamate, A. Saruwatari, A. Nakanishi, Y. Matsumae, K. Ueno, K. Dokko, and M. Watanabe, *Electrochem. Commun.*, 109 (2019) 106598.
23. T. Kun-Ju, N. Chung-Sheng, C. Han-Yi, and H. Jin-Hua, *J. Power. Sources.*, 454 (2020) 227912.
24. K. Joel, Q. Yan, and Z. Linghong, *J. Power. Sources*, 450 (2020) 227711.
25. N. Biljana, J. Sandra, and M. Iva, *Talanta*, 164 (2017) 201-208.
26. R. Ouyang, Z. Zhu, C.E. Tatum, J.Q. Chambers, and Z.L. Xue, *J. Electroanal. Chem.*, 656 (2011) 78.
27. B.M. Abad, D. Izquierdo, L. Perez, I. Escudero, and M.J.A. Martínez, *Talanta*, 182 (2018) 549.
28. R. Chokkareddy, T. Niranjan, and G.G. Redhi, Green Sustainable Process for Chemical and Environmental Engineering and Science, (2020) 367.
29. E. Molaakbari, A. Mostafavi, and Z. *J. Electroanal. Chem.*, 801 (2017) 198.
30. L.Yixia, H. Jian, and Z. Yanbo, *Sens. Actuators, B*, 311 (2020) 127911.
31. A. Khoshroo, L. Hosseinzadeh, A. Sobhani-Nasab, and M. Rahimi-Nasrabadi, *Microchem. J.*, 145 (2019) 1185.
32. A. Abo-Hamad, M.A. AlSaadi, M. Hayyan, I. Juneidi, and M.A. Hashim, *Electrochim. Acta*, 193 (2016) 321.
33. Y. Lin, L. Jingyuan, and Y. Wenyan, *Talanta*, 209 (2020) 120515.
34. E. Nagles, O. García-Beltrán, and J.A. Calderónb, *Electrochim. Acta*, 258 (2017) 512.
35. P. Shirley, J.G. Annathea, and P. Alyson, *Sensing and Bio-Sensing Research*, 23 (2019) 100268.
36. S. Chaiyo, E. Mehmeti, K. Žagar, W. Siangproh, O. Chailapakul, and K. Kalcher, *Anal. Chim. Acta*, 918, (2016) 26.
37. X. Chen, C.A. Yuan, C.Wong, and S.W.Koh, *Mol. Simul.*, 37 (2011) 990.
38. Z. Liu, B. Lu, H. Xiao, D. Liu, and L. Nagorskaya, *Environ. Pollut., Ser. A.*, 254 (2019) 112968.
39. R.J. Soukup-Hein, M.M. Warnke, and D.W. Armstrong, *Annu. Rev. Anal. Chem.*, 2 (2009) 145.
40. C. Soares, J.A.T. Machado, M.L. António, *Food Chemistry*, 302 (2020) 125345.
41. R. Xu, X.Y. Yu, C. Gao, Y.J. Jiang, D.D. Han, and J.H. Liu, *Anal. Chim. Acta*, 790 (2013) 31.
42. C. Pérez-Ràfols, J. Bastos-Arrieta, and N. Serrano, *Sensors*, 17 (2017) 6.

43. V. Sosa, C. Barceló, N. Serrano, C. Ariño, J.M. Díaz-Cruz, and M. Esteban, *Anal. Chim. Acta*, 855 (2015) 32.
44. C. Li, X. Zhao, and X. Han, *Anal. Methods.*, 10 (2018) 4945.
45. Y.G Lee, and A. Jang, *J. Coastal Res*, 79 (2017) 45.
46. P.F. Niu, C.F. Sanchez, M. Gich, C.N. Hernandez, and P.F. Bolado, *Microchim. Acta*, 183 (2016) 617.
47. H. Wang, G. Zhao, Z. Zhang, Y. Yi, Z. Wang, and G. Liu, *Int. J. Electrochem. Sci*., 12 (2017) 4702.
48. N. Promphet, and P. Rattanarat, *Sens. Actuators B*, 207 (2015) 526.
49. N. Lezi, A. Economou, P.A. Dimovasilis, P.N Trikalitis, and M.I. Prodromidis, *Analytica. Chimica. Acta*, 728 (2012) 1.
50. C. Kokkinos, A. Economou, I. Raptis, and C.E. Efstathioua, *Electrochim. Acta*, 53 (2008) 5294.